The α-boron cages with four-member rings

2009 EPL 85 68005

(http://iopscience.iop.org/0295-5075/85/6/68005)

A Letters Journal Exploring the Frontiers of Physics

March 2009

EPL, **85** (2009) 68005
doi: 10.1209/0295-5075/85/68005

www.epljournal.org

The α-boron cages with four-member rings

Rajendra R. Zope

Department of Physics, The University of Texas at El Paso - El Paso, TX 79958, USA

received 19 December 2008; accepted in final form 20 February 2009
published online 1 April 2009

PACS 81.05.Tp – Fullerenes and related materials
PACS 61.48.-c – Structure of fullerenes and related hollow molecular clusters
PACS 61.46.Km – Structure of nanowires and nanorods (long, free or loosely attatched, quantum wires and quantum rods, but not gate-isolated embedded quantum wires)

Abstract – A new class of $32n^2$ boron cages which are made closed by six squares is proposed and a procedure to build such cages using an α-boron sheet is described. Each member from this infinite set of boron cages has a structure that is compatible with the most stable α-boron sheet that maintains an optimal balance of the two-center and three-center bonds. Accurate density functional calculations with a large polarized Gaussian basis set show that B_{32}, B_{96}, B_{128}, and B_{288} are energetically stable structures. The smallest B_{32} cage from this class has the HOMO-LUMO gap of 1.32 eV, the largest amongst the boron cages and boron fullerenes studied so far.

Since the observation of carbon fullerenes, the question whether its preceding neighbor, boron, can form fullerene-like structures has intrigued several researchers [1–11]. In the last two years, significant progress has been made towards the understanding of the boron nanostructures [12]. During the last two years stable nanostructures of boron such as fullerenes [13–15], onions [16], planar sheets [12,17,18], and nanotubes [17,19–21] have been proposed. Yakobson and coworkers using density functional calculations showed that an 80-atom fullerene composed entirely of boron is stable [13]. The B_{80} fullerene has structural resemblance with the C_{60} fullerene. Like C_{60}, it has 12 pentagons and 20 hexagons, with the 20 additional boron atoms capping the hexagonal rings. Its stability was explained in terms of its structure, which consists of six interwoven double-ring clusters [13].

In a subsequent work, Tang and Ismail-Beigi and Yang *et al.* predicted the existence of a new class of boron sheets containing triangular and hexagonal motifs [12,17]. These sheets are the most stable boron sheets found to date. These sheets are obtained either by removing atoms from the triangular boron sheets or by putting atoms in the hexagonal sheets. The number of ways the atoms can be inserted in the hexagonal sheet is very large. Tang and Ismail-Beigi investigated the energetics of the boron sheets with a different distribution of holes and noted that the boron sheet with *evenly distributed* holes is the most stable one. The holes (hexagonal rings with missing center atoms) are distributed in such a way that each hole is isolated from the other holes by hexagonal rings with central atoms. Furthermore, each hexagonal ring with a central atom has three holes as neighbors arranged in an alternate fashion. They called the boron sheet with such pattern of holes as α-boron sheet. A piece of α-boron sheet is shown in fig. 1. The enhanced stability of these boron sheets is due to the balance of two-center and three-center bonding. The nanotubes obtained by curling up these sheets are the most stable boron nanotubes noted

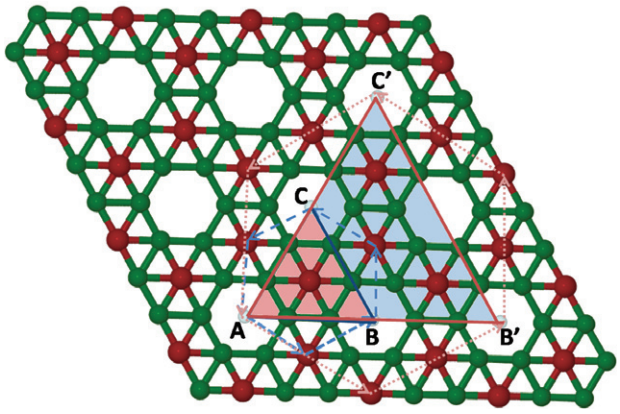

Fig. 1: (Color online) The α-boron sheet. The atoms colored in green form the hexagonal sheet. Both the parent octahedral cages and α-boron cages can be obtained using the equilateral triangular patches. For example, the triangles ABC and AB′C′ when pasted on octahedron faces will lead to octahedral B_{24} and B_{96} parent cages if a hexagonal framework is used, and to B_{32} and B_{128} α-boron cages when an α-boron sheet is used.

so far [17,20]. The bonding picture proposed to explain the stability of boron sheets incidentally also provides an explanation for the stability of the B_{80} fullerene. Its stability is due to an optimal balance of the 12 electron-deficient pentagonal rings and 20 electron-rich hexagonal rings. In this letter, we present a new class of closed boron cages which like B_{80} are interlocked double-rings boron clusters [14] and are compatible with the most stable hole-doped α-boron sheets [12]. These α-boron cages are energetically competitive with the B_{80} fullerene. The B_{32} α-boron cage from this new class is the smallest closed cage that can be obtained from the most stable hole-doped α-boron sheets. The all-electron density functional calculations show that it has the largest gap between the highest occupied molecular orbital and the lowest unoccupied molecular orbital amongst all boron fullerenes studied so far.

The C_{60} fullerene can be generated from hexagons (graphene sheet) by introducing defects. These defects are the fivefold pentagonal rings which introduce curvature in the graphene sheet. The Euler polyhedron theorem indicates that exactly 12 pentagons are required to form a closed hollow fullerene. The B_{80} fullerene can be similarly obtained from the hole-doped α-boron sheet. The B_{80} is the smallest fullerene in which pentagonal rings are isolated from each other. The closed-cage structures can also be obtained using fourfold rings (*i.e.* squares) as defects rather than fivefold pentagonal rings. By using the Euler theorem on polyhedra it is trivial to show that exactly 6 fourfold rings are required to form a cage structure [22]. If the polyhedron (cage) has N vertices (atoms), E edges, and F faces, then $N + F = E + 2$. Thus, the number of defects (four-member rings) are 6, fewer than 12 defects (pentagonal rings) required to generate fullerenes. In carbon fullerenes, the fullerenes which have defects, as far as possible, are energetically the most favorable structures. This is the so-called *isolated pentagon rule* [23]. A similar six-square rule has been proposed by Slanina and coworkers for the boron nitride cages obtained using six squares [22]. The six defects (four-member rings) in the infinite class of α-boron cages proposed in this work also are arranged in symmetric fashion as far as possible from each other.

The $32n^2$ α-boron cages proposed in this work can be built from the α-boron sheet using a procedure akin to that used by Zhu *et al.* to construct $24n^2$ parent boron cages from a hexagonal sheet [24]. As illustrated in fig. 1, the $32n^2$ α-cages are built by cutting out equilateral triangles from the α-boron sheet and pasting them on the 8 faces of an octahedron. The triangles are obtained by taking steps in directions which are 120° from each other. The steric repulsion between boron atoms dictates that the most stable cages will have holes at the 6 corners of the octahedron. For example, to obtain the smallest B_{32} cage we take 2 steps: first, starting from the center of the *hole* (hollow hexagon, point A in fig. 1) to the center of the adjacent hexagon and the second step at 120° to the center

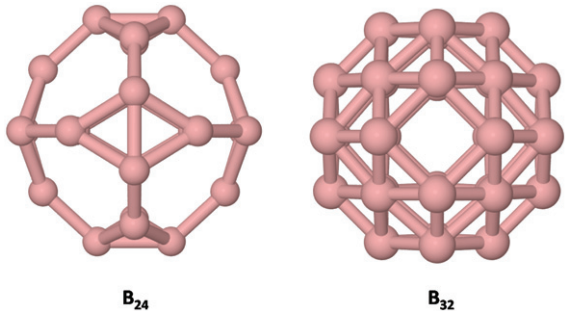

Fig. 2: (Color online) The smallest member of the $24n^2$ octahedral B_{24} cage (left) and the corresponding smallest member of the $32n^2$ B_{32} α-boron cage (right) derived from the parent B_{24} cage.

of the hole (point B). The path of these steps is shown by the dashed line. This defines an edge of equilateral triangle. Three such (1,1) steps will give an equilateral triangle ABC (colored red in fig. 1). The apices of ABC are (1,1) steps away where the steps are taken along the directions that are 120° apart. The next member B_{128} of the $32n^2$ class is obtained by taking (2,2) steps to reach the apices of the triangles. Equal steps in the two directions will result in holes at the apices of the triangle. The resultant equilateral triangle $AB'C'$ can be used to construct the B_{128} α-cage. This procedure can be repeated to obtain larger triangles which can in turn be used to construct larger members of an infinite class of $32n^2$ α-boron cages. If the triangles are cut from the hexagonal sheet (the atomic framework depicted in green in fig. 1) one gets the $24n^2$ class of octahedral parent boron cages [24]. The (n, n) equilateral triangle cut from the α-boron sheet has exactly n^2 additional boron atoms (at the center of the hexagons) with respect to the corresponding (n, n) equilateral triangle cut from the graphene sheet. Thus, the addition of $8n^2$ atoms from the 8 equilateral triangles results in the $32n^2$ class of α-boron cages that is related to the $24n^2$ class of the parent boron cages. The smallest member of the $32n^2$ α-boron cages, the B_{32} cage, is shown in fig. 2, along with its parent B_{24} cage (the smallest member of the $24n^2$ parent boron cages).

As the α-boron cages are designed from the α-boron sheet, the optimal balance between the electron-rich and electron-deficient region is maintained as in the sheet. The larger members B_{128} and B_{288} of the $32n^2$ class and the corresponding B_{96} and B_{216} members from the parent $24n^2$ class of boron cages are shown in fig. 3. While this work is about the $32n^2$ boron cages, we have also included the B_{96} α-boron cage outside this class. In this letter we demonstrate, by performing all-electron density functional calculations on B_{32}, B_{96}, B_{128}, and B_{288} cages, that the α-boron cages containing four-member rings are stable structures. Our goal is to demonstrate that the members of the proposed infinite class of $32n^2$ α-boron cages are stable structures and not to identify lowest-energy structures.

The present calculations performed in this spirit and using a large polarized Gaussian basis set indicate that

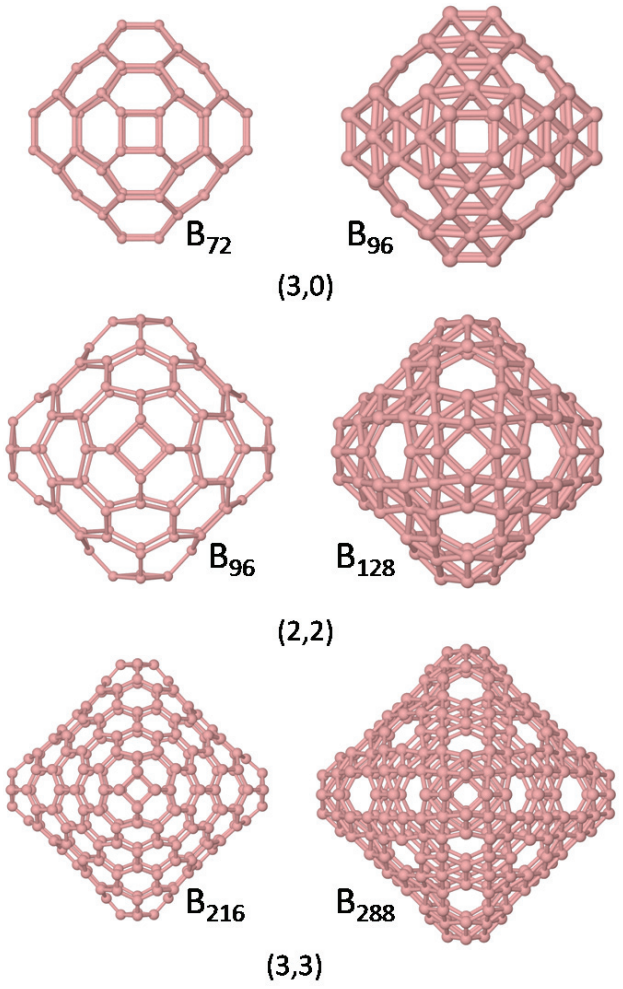

Fig. 3: (Color online) The B_{96}, B_{128}, and B_{288} α-boron cages. The parent B_{72}, B_{96}, and B_{216} parent boron cage structures are shown on the left. The numbers in bracket refer to the indices m and n corresponding to the steps taken on the α-boron sheet to build cages (see text for more details).

these cages are electronically closed-shell systems and are energetically stable structures. The vibrational analysis on the smallest member shows that it is vibrationally stable. The B_{128} and B_{288} α-boron cages are the most stable boron cages reported so far. A very recent work by Yan *et al.* that appeared during the preparation of this manuscript shows a different approach based on the modified leapfrog algorithm to generate α-boron cages [25].

Our calculations are performed using the NRLMOL suit of codes which implements the Kohn-Sham formulation of the density functional theory using the linear combination of the Gaussians-type scheme [26–28]. For accurate calculations, we employ a large polarized Gaussian basis set with 35 basis functions per atom to express molecular orbitals [29,30]. Each basis function is obtained by contraction of 12 primitive Gaussians. Accurate numerical grids are used to obtain the exchange correlation contributions to the Hamiltonian matrix and energy. The exchange correlation effects are described at the generalized gradient approximation level using the Perdew-Burke-Ernzerhof model [31]. The equilibrium boron cage structures are obtained by optimizing the atomic positions until the forces on atoms were less than 10^{-3} hartree/bohr.

As mentioned earlier, the smallest cage that can be built from the hexagonal sheet using six-square defects is the 24-atoms truncated octahedron (cf. fig. 1), which is also the geometry of the sodalite cage of ultramarines. It consists of six fourfold rings (squares) separated by the eight hexagonal rings and has an O_h point group symmetry. The parent B_{24} cage is a stationary point on the potential energy surface. The vibrational analysis, however, indicates that it is not a minimum (vibrationally stable). It has three triply degenerate unstable vibrational modes. The B_{32} α-cage, like the T_h B_{80} fullerene [15,32] has three inequivalent atoms: 2 generate the parent B_{24} cage and the third generates the atoms at the center of the hexagons. The vibrational frequencies of the B_{32} α-cage are real. Thus, the cage structure is vibrationally stable. The binding energy of the B_{32} α-cage is 5.35 eV/atom, less than that of the B_{80} fullerene (5.85 eV/atom). Boustani *et al.* [33] and Zhao *et al.* [34] have studied the energetics of B_{32} clusters which also includes the B_{32} α-cage. In both studies the B_{32} α-cage is found to be the most stable cage structure. The symmetry of the B_{32} cluster is reported to be lower than the octahedral symmetry found in this work. Our calculations show that the B_{32} α-cage is vibrationally stable with octahedral symmetry. Both these studies (Boustani *et al.* and Zhao *et al.*) show that at this size, the ring structure is energetically favorable over cages. It will be interesting to investigate the exact cluster size at which the cage structures become energetically more favorable. This crossover occurs before B_{80} [13]. Using the Hartree-Fock approximation and the 3–21G basis, Boustani *et al.* obtained the binding energy of the B_{32} α-cage to be 3.10 eV/atom. This is more than 2 eV/atom smaller than the present value (5.35 eV/atom). The difference is due to the lack of correlation treatment and the use of a small basis set by Boustani *et al.*

The B_{32} α-cage is special in that it has the largest HOMO-LUMO gap (1.32 eV) of all the boron cage structures including boron fullerenes [14] and onions [16]. The HOMO-LUMO gap approximates the chemical hardness which is a measure of chemical reactivity. So the B_{32} α-cage should be chemically less reactive than the B_{80} fullerene. Its smaller binding energy is probably the consequence of the increased curvature due to its smaller size. Increasing the size of the B_{32} α-cage by introducing more hexagons increases the binding energy of the boron cage. The larger size reduces the strain due to curvature and also results in a larger fraction of atoms being in an α-boron-sheet–like environment. The B_{96} α-cage has a binding energy of 5.82 eV/atom and is energetically competitive with the B_{80} fullerene [15]. The B_{96} α-cage is outside the $32n^2$ class but can be

Table 1: The binding energy per atom (BE), the highest occupied molecular orbital (HOMO) eigenvalue ϵ_{HOMO}, the lowest unoccupied molecular orbital (LUMO) eigenvalue ϵ_{LUMO}, and the HOMO-LUMO gap Δ, of α-boron cages, and the B_{80} fullerene [15]. The BE of the most stable α-boron sheet from ref. [12] is given in the last row. All energies are in eV.

		BE	$-\epsilon_{HOMO}$	$-\epsilon_{LUMO}$	Δ
B_{32}	O_h	5.35	5.36	4.04	1.32
B_{96}	T_d	5.82	5.06	4.04	1.02
B_{128}	T_h	5.87	4.85	4.26	0.6
B_{288}	T_h	5.94	4.58	4.53	0.05
B_{80}	T_h	5.85	5.22	4.25	0.96
α-sheet	–	6.11	–	–	–

Table 2: The range of bond lengths in α-boron cages. All values are in Å. The description of the bonds is given in the text. The bond lentghs in the α-boron sheet are in the range 1.66–1.9 Å [12].

	$(6',6')$	$(6,6')$	$(4,6')$	$(c,6')$
B_{32}	1.64	–	1.78	1.71
B_{96}	1.65–1.76	1.73	1.74	1.68–1.73
B_{128}	1.68–1.73	1.71–1.72	1.74	1.68–1.73
B_{288}	1.68–1.73	1.71–1.72	1.74	1.68–1.73

obtained from the B_{32} α-cage by inserting 32 hexagons, of which, 24 have a central atom. Alternatively, it can be obtained from the parent T_d B_{72} cage by capping the hexagons so that its structure is compatible with the most stable boron sheet. The HOMO-LUMO gap of the B_{96} cage is 1.02 eV larger than that of B_{80} (0.97 eV). We also computed the B_{96} ring structure using the same computational methodology. The B_{96} ring structure is 5.7 eV less stable than the B_{96} α-cage. The inspection of the electronic structure of the optimized larger B_{128} and B_{288} α-cages indicate that both cages are closed-shell systems with a HOMO-LUMO gap of 1.02, 0.05 eV, respectively. The very small (0.05 eV) gap of the B_{288} α-cage is consistent with the metallic nature of the α-boron sheet [12]. The properties of the α-cages in the infinite limit should approach to those of the α-boron sheet. The B_{128} and B_{288} α-cages have binding energies of 5.87 and 5.94 eV/atom, respectively. The HOMO-LUMO gaps and binding energies of all cages are summarized in table 1.

The binding energy increases in larger boron cages due to the decrease in curvature and due to the larger fraction of the boron atoms being in an environment similar to that of the α-boron sheet. For extremely large cages the binding energy should be close to the cohesive energy of the α-boron sheet.

In the α-boron cages, the bond distances are of four types: i) the bonds shared by two hexagonal rings with central boron atoms $(6',6')$; ii) the bonds shared by a hexagonal ring and by a hexagonal ring with central atom $(6,6')$; iii) the bonds shared by four-member rings and a hexagonal ring with central atom $(4,6')$; iv) the bond between the central atom in a $(6',6')$ ring and the six boron atoms on the ring. (We will call this $(c,6')$ bond for convenience.) We use the prime to distinguish between the hexagonal rings with and without central atom. The $6'$ refers to a hexagonal ring with a boron atom at its center. The bond distances are summarized in table 2. In the case of B_{80} (and other boron fullerenes) the $(5,6')$ bond is 1.74 Å, larger than that of $(6',6')$, 1.67 Å [15]. Thus, bond alternation like in C_{60} is also seen in B_{80}. Such a trend is also observed in the $32n^2$ class of α-boron cages, as can be seen in table 2. The inspection of eigenvalues of α-boron cages shows that the HOMO is threefold degenerate while the LUMO is nondegenerate except for B_{32} and B_{96} cages in which it is triply degenerate. The isosurface plots of the HOMO and LUMO orbital densities are given in fig. 4. In all α-boron cages the HOMO density is always localized on the shorter $(6',6')$ bonds. The LUMO density is mostly concentrated on bonds shared by the four-member ring (defect) and the hexagon ($(4,6')$ bonds). This pattern is similar to that in the case of the B_{80} fullerene in which the HOMO density is mostly on the shorter $(6',6')$ bond and the

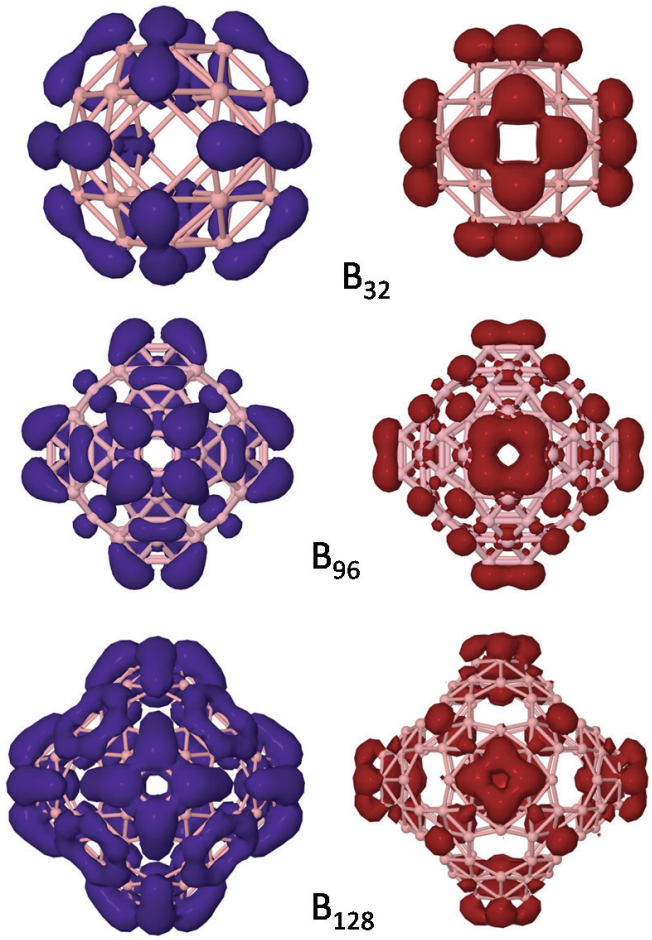

Fig. 4: (Color online) The HOMO (left) and LUMO (right) orbital densities of B_{32}, B_{96}, and B_{128} α-boron cages.

LUMO density on the longer $(5, 6')$ bonds shared by the pentagonal ring (defect for fullerene) and the hexagonal ring [15].

To summarize, an infinite class of $32n^2$ α-boron cages that is related to a $24n^2$ class of *parent* boron cages is proposed. The procedure to build the $32n^2$ α-boron cages directly from the most stable α-boron sheet is illustrated. The accurate density functional calculations using large polarized Gaussian basis sets containing 35 basis functions per atoms are performed to demonstrate the stability of the B_{32}, B_{128}, and B_{288}, the smallest 3 members from the infinite class of the $32n^2$ α class and the B_{96} α-boron cage outside this class. The calculations show that the proposed α-boron cages are energetically stable structures. The result that larger α-boron cages are more stable than the B_{80} fullerene is also consistent with a recent report which shows the construction of boron *fullerenes* from smaller fullerenes using the modified leapfrog transformation [25].

The present work may have implications in cancer therapy as boron species have been used in cancer treatment [35]. Boron-based semiconducting materials have possible applications as solid-state neutron detectors. Hence, like B_{80}-based solids [36,37], it will be interesting to explore the possibility of obtaining boron-rich semiconductors using α-boron cages as building blocks.

* * *

The author acknowledges discussions with Dr T. Baruah, the Texas Advanced Computing Center (TACC-AUSTIN, USA) for computational support.

REFERENCES

[1] Dadashev V., Gindulyte A., Lipscomb W. N., Massa L. and Squire R., *Struct. Mech. Ashes Enzym.*, **827** (2002) 79.
[2] Derecskeikovacs A., Dunlap B. I., Lipscomb W. N., Lowrey A., Marynick D. S. and Massa L., *Inorg. Chem.*, **33** (1994) 5617.
[3] Gindulyte A., Krishnamachari N., Lipscomb W. N. and Massa L., *Inorg. Chem.*, **37** (1998) 6546.
[4] Boustani I., Quandt A., Hernández E. and Rubio A., *J. Chem. Phys.*, **110** (1999) 3176.
[5] Chacko S., Kanhere D. G. and Boustani I., *Phys. Rev. B*, **68** (2003) 035414.
[6] Boustani I. and Quandt A., *Europhys. Lett.*, **39** (1997) 527.
[7] Quandt A. and Boustani I., *ChemPhysChem.*, **6** (2005) 2001.
[8] Evans M. H., Joannopoulos J. D. and Pantelides S. T., *Phys. Rev. B*, **72** (2005) 045434.
[9] Kunstmann J. and Quandt A., *Phys. Rev. B*, **74** (2006) 035413.
[10] Boustani I., *J. Solid State Chem.*, **133** (1997) 182.
[11] Lau K. C. and Pandey R., *J. Phys. Chem. C*, **111** (2007) 2906.
[12] Tang H. and Ismail-Beigi S., *Phys. Rev. Lett.*, **99** (2007) 115501.
[13] Szwacki N. G., Sadrzadeh A. and Yakobson B. I., *Phys. Rev. Lett.*, **98** (2007) 166804.
[14] Gonzalez Szwacki N., *Nanoscale Res. Lett.*, **3** (2008) 49.
[15] Baruah T., Pederson M. R. and Zope R. R., *Phys. Rev. B*, **78** (2008) 045408.
[16] Prasad D. L. V. K. and Jemmis E. D., *Phys. Rev. Lett.*, **100** (2008) 165504.
[17] Yang X., Ding Y. and Ni J., *Phys. Rev. B*, **77** (2008) 041402, http://link.aps.org/abstract/PRB/v77/e041402.
[18] Lau K. C. and Pandey R., *J. Phys. Chem. B*, **112** (2008) 10217, http://pubs.acs.org/doi/abs/10.1021/jp8052357.
[19] Kunstmann J. and Quandt A., *Phys. Rev. B*, **74** (2006).
[20] Singh A. K., Sadrzadeh A. and Yakobson B. I., *Nano Lett.*, **8** (2008) 1314.
[21] Lau K. C., Orlando R. and Pandey R., *J. Phys.: Condens. Matter*, **20** (2008) 125202; Lau K. C., Pandey R., Pati R. and Karna S. P., *Appl. Phys. Lett.*, **88** (2006) 212111.
[22] Sun M.-L., Slanina Z. and Lee S.-L., *Chem. Phys. Lett.*, **233** (1995) 279.
[23] Schmalz T. G., Seitz W. A., Klein D. J. and Hite G. E., *J. Am. Chem. Soc.*, **110** (1988) 1113, http://pubs.acs.org/doi/abs/10.1021/ja00212a020.
[24] Zhu H. Y., Klein D. J., Seitz W. A. and March N. H., *Inorg. Chem.*, **34** (1995) 1377.
[25] Yan Q.-B., Sheng X.-L., Zheng Q.-R., Zhang L.-Z. and Su G., *Phys. Rev. B*, **78** (2008) 201401, http://link.aps.org/abstract/PRB/v78/e201401.
[26] Pederson M. R. and Jackson K. A., *Phys. Rev. B*, **41** (1990) 7453.
[27] Jackson K. and Pederson M. R., *Phys. Rev. B*, **42** (1990) 3276.
[28] Pederson M. R. and Jackson K. A., *Phys. Rev. B*, **43** (1991) 7312.
[29] Porezag D. and Pederson M. R., *Phys. Rev. A*, **60** (1999) 2840.
[30] Porezag D. and Pederson M. R., *Phys. Rev. B*, **54** (1996) 7830.
[31] Perdew J. P., Chevary J. A., Vosko S. H., Jackson K. A., Pederson M. R., Singh D. J. and Fiolhais C., *Phys. Rev. B*, **48** (1993) 4978.
[32] Gopakumar G., Nguyen M. T. and Ceulemans A., *Chem. Phys. Lett.*, **450** (2008) 175.
[33] Boustani I., Rubio A. and Alonso J. A., *Chem. Phys. Lett.*, **311** (1999) 21.
[34] Zhao Y.-y, Zhang M.-y, Chen B.-g, Zhang J. and Sun C.-C., *J. Mol. Struct.: THEOCHEM*, **759** (2006) 25.
[35] Hawthorne M. F. and Maderna A., *Chem. Rev.*, **99** (1999) 3421, http://pubs.acs.org/doi/abs/10.1021/cr980442h.
[36] Liu A. Y., Zope R. R. and Pederson M. R., *Phys. Rev. B*, **78** (2008) 155422, http://link.aps.org/abstract/PRB/v78/e155422.
[37] Yan Q.-B., Zheng Q.-R. and Su G., *Phys. Rev. B*, **77** (2008) 224106.